

Surface states and oxygen chemisorption on Ti(0001)

B. T. Jonker, J. F. Morar, and Robert L. Park

Department of Physics and Astronomy, University of Maryland College Park, Maryland 20742

(Received 8 May 1981)

The system O₂ on Ti(0001) has been investigated using appearance potential spectroscopy (APS), Auger electron spectroscopy (AES), low-energy electron diffraction (LEED), and work-function measurements obtained by the field-emission retarding potential technique. A strong band of states just above the Fermi level was found to be localized near the surface. This band of surface states broadened with increasing temperature and was suppressed by exposure to oxygen. Although weaker, a similar band of surface states was previously observed on polycrystalline titanium samples and more recently predicted for the (0001) surface to occur at the Fermi level and to extend a few tenths of an eV on either side of it [Peter J. Feibelman, J. A. Appelbaum, and D. R. Hamann, *Phys. Rev. B* **20**, 1433 (1979)]. The sensitivity of the surface-state signal to sampling depth was demonstrated by continuously varying the sampling depth between the 5–10 Å inelastic mean free path of the incident electrons in Auger electron appearance potential spectroscopy and approximately half that value for disappearance potential spectroscopy. The work function remained approximately constant for very low oxygen coverage and then steadily increased with additional exposure from a clean-surface value of 4.58 ± 0.05 eV, leveling off at approximately 5.3 eV as the surface became saturated with oxygen. The initially diffuse low-coverage $p(2 \times 2)$ LEED superstructure formed upon exposure at room temperature was significantly improved upon flashing the sample to 250°C. This was accompanied by an abrupt decrease of 0.15 eV in the work function, although AES revealed no decrease in the amount of oxygen on the surface. A similar decrease in the work function upon a 250°C flash anneal was observed for other exposures as well, suggesting some reordering of the surface adatoms. These results are interpreted in terms of two chemisorption states for the oxygen: a tightly bound α state at low coverages characterized by a well-ordered $p(2 \times 2)$ LEED pattern and a work function below that of the clean surface, and a β state characterized by a disordered structure and a work function higher than the clean surface value. Heating converts the β state to the α state.

I. INTRODUCTION

Recent progress in computational techniques now enables self-consistent calculations to be made of the surface electronic structure of d -band materials.¹ In a recent publication Feibelman, Appelbaum, and Hamann calculated the layer-by-layer electronic structure of an 11-layer Ti(0001) film.² Figure 1 shows a plot of the local density of states (LDOS) vs layer for the first six layers taken from their publication. A very prominent peak in the density of states of the first layer lies at the Fermi level, extending a few tenths of an eV on either side of it. Proceeding into the film there is a significant change in the LDOS between the first and second layers, but little change as one proceeds past the second layer, indicating that the density of states very quickly assumes its bulk structure as one moves in

from the surface, in fact, almost by the second layer.

Although the Fermi level nearly corresponds to a local minimum or dip in the LDOS a few layers from the surface, it nearly coincides with an absolute maximum in the first layer. Such a prominent feature should be observable in any surface-sensitive spectroscopy that probes either the filled or the unfilled states, since the peak in the local density of states in the first layer of the film extends on either side of the Fermi energy. Indeed, a band of states lying just above the Fermi level of polycrystalline titanium was observed in the titanium $2p_{3/2}$ appearance potential spectrum prior to the prediction of Feibelman *et al.*^{3–5} This band of states, which appears as a shoulder on the leading edge of the first-derivative appearance potential spectrum (Fig. 2), was shown to be very sensitive to a variety of gases,

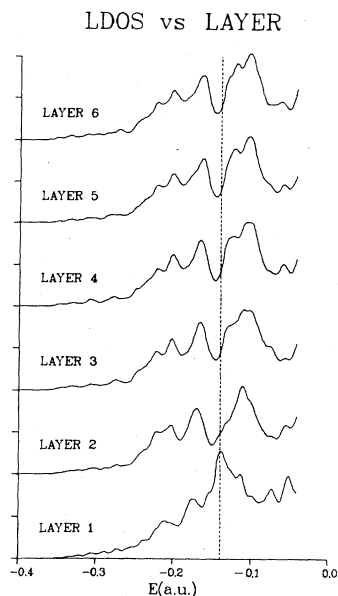


FIG. 1. Layer-by-layer local density of states (LDOS) for an 11-layer Ti(0001) film. The energy zero is at the vacuum level. The dotted line indicates the Fermi level at $E = -0.139$ a.u. ($= -3.8$ eV). Note the strong surface resonance in the outermost ("1st") layer. From Ref. 2 by permission.

including oxygen.^{4,5} As gas atoms adsorbed on the surface, the electronic structure of the titanium surface was continuously altered in such a way as to extinguish the band of states producing the shoulder. It seems probable that these states correspond to

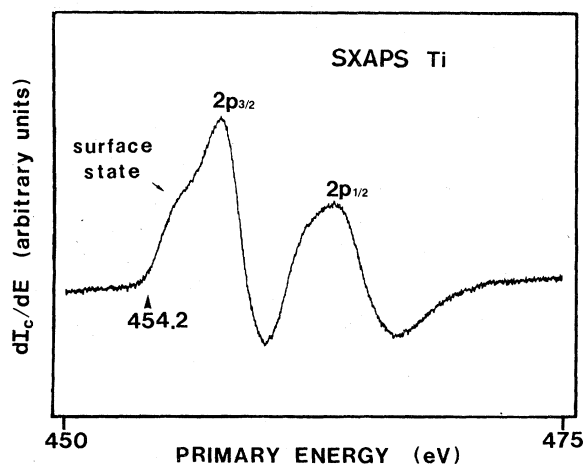


FIG. 2. First-derivative soft-x-ray appearance potential spectrum of the $2p$ levels of polycrystalline Ti, obtained using a field-emission array electron source and nude surface barrier detector. For polycrystalline Ti, the surface states appear as a shoulder on the leading edge of the $2p_{3/2}$ peak.

the unfilled portion of the surface band calculated by Feibelman *et al.*² for the basal plane. Subsequent to the theoretical predictions of Feibelman *et al.*,² Feibelman and Himpsel observed a strong band of filled states at the Fermi level of a clean Ti(0001) surface which was extinguished by exposure to hydrogen.⁶ The observation of surface states in filled bands is, of course, not new, but there have been few such observations in the unfilled bands. Therefore, in the experiments described here we use appearance potential spectroscopy (APS) to investigate the states above the Fermi level of the clean Ti(0001) surface and their change with exposure to oxygen. The surface was characterized during these measurements by low-energy electron diffraction (LEED), Auger-electron spectroscopy (AES), and work-function measurements.

II. EXPERIMENTAL

Appearance potential spectroscopy measures the probability for the creation of excited core states of atoms in the surface region of a solid by electron bombardment.⁷ Above a core excitation threshold, this probability depends on the states available to two electrons. Assuming constant matrix elements, the electron excitation probability $N_{\beta}(E)$ will vary as the self-convolution of the one-electron density of unfilled states, broadened by the Auger lifetime of the core hole, i.e.,

$$N_{\beta}(E) = N(E) * N(E) * \rho(E + E_B), \quad (1)$$

where $N(E)$ is the density of unfilled states, E_B is the core binding energy, and $\rho(E)$ is a Lorentzian of the form

$$\rho(E) = \frac{1}{\pi} \frac{\Gamma}{E^2 + \Gamma^2}. \quad (2)$$

Γ is related to the core-hole lifetime τ by

$$\Gamma = \hbar/\tau. \quad (3)$$

The self-convolution in Eq. (1) obscures much of the detail in $N(E)$. This detail is recovered in part by plotting the derivative of $N_{\beta}(E)$,

$$\frac{dN_{\beta}(E)}{dE} = \frac{dN(E)}{dE} * N(E) * \rho(E + E_B). \quad (4)$$

To the extent that $dN(E)/dE$ is dominated by the Fermi discontinuity, it can be approximated by a delta function

$$\frac{dN(E)}{dE} \simeq N(E_F)\delta(E), \quad (5)$$

where $N(E_F)$ is a constant determined by the density of states at the Fermi level. With this substitution, Eq. (4) can be integrated to yield

$$\frac{dN_{\beta}(E)}{dE} \simeq N(E_F)[N(E) * \rho(E + E_B)]. \quad (6)$$

Thus the derivative of the electron excitation function should resemble the one-electron density of unfilled states broadened by the core-hole lifetime. This approximation is best for free-electron-like metals. For transition metals $N(E)$ exhibits a strong peak at E_F , resulting in a derivative spectrum that exhibits a pronounced undershoot following the threshold peak.

APS can assume several forms, depending upon the signal one chooses to detect.⁸ Each form, however, conveys essentially the same information. For reasons of convenience we chose to use disappearance potential spectroscopy^{8,9} (DAPS) and Auger-electron appearance potential spectroscopy (AEAPS) for this study.

The experiments were conducted in a sputter-ion-pumped stainless-steel vacuum system with a base pressure of less than 10^{-10} Torr. Extensive cleaning procedures as described in the literature were necessary to produce a clean surface as determined by LEED and AES,¹⁰ and only after many cycles of Ar^+ -ion bombardment and annealing at 750 °C were the best results obtained. The sample could be heated by an indirect resistive heater, and the temperature was monitored via a Chromel-Constantan thermocouple attached to the sample. All exposures were made at room temperature by the dynamic flow method at an oxygen partial pressure of 10^{-8} Torr as measured by a nude ionization gauge calibrated for nitrogen. No corrections for this calibration were made. AES was used to measure the actual relative amount of oxygen on the surface (primary energy 1.5 keV, modulation 2 V rms). All AES and APS spectra were obtained using a commercial 4-grid LEED apparatus. Disappearance potential spectra were recorded using a 0.2-V rms modulation and 400 millisecond time constant (spectra obtained while heating the sample required a 1.25-sec time constant to reject line noise contributed by the heater). Auger electron appearance potential spectra were recorded using a 0.1-V rms modulation and 1.25-sec time constant. The maximum current density incident on the sample was approximately $20 \mu\text{A}/\text{mm}^2$; no evidence was seen for significant electron-induced desorption of the oxygen by the primary electron beam. AES together with LEED observations enabled an estimate

of absolute coverage to be made as described in later paragraphs.

III. CLEAN Ti(0001) SURFACE

In its simplest form the appearance potential spectrum is determined from the increase in the total secondary electron yield above the core excitation threshold resulting from Auger recombination of the core hole (AEAPS). Most of this change, however, is contributed by low-energy secondaries produced by stopping the characteristic Auger electrons.⁸ The sampling depth in this case is determined by the inelastic mean free path of the incident electrons. At the energy of the $2p_{3/2}$ threshold (454.2 eV) this is about $5-10 \text{ \AA}$.¹¹

It is, however, also possible to extract the appearance potential spectrum from the quasielastic electron yield (DAPS), which *decreases* above the threshold due to the opening of a new channel for inelastic scattering. As Kirschner and Staib¹² have noted, this results in a sampling depth approximately half as great as in AEAPS since the quasielastic electrons must travel both directions without scattering inelastically. One can in fact continuously adjust the sampling depth between these limits by setting a high-pass energy analyzer to admit electrons which have lost increasing amounts of energy.

This is illustrated in Figs. 3 and 4. Figure 3 shows a series of first-derivative spectra of the clean Ti(0001) surface taken for high-pass threshold energies of 0, 2, 4, and 10 eV below the incident electron energy (apart from a correction for the work function of the spectrometer). In the top spectrum one is detecting only the very nearly elastic secondaries, consequently emphasizing surface features. Note that where there was once a shoulder in the polycrystalline spectrum (Fig. 2), there is now a very prominent surface-state peak, even larger than the $2p_{3/2}$ bulk peak. The separation in energy of these two peaks is 1.8 eV, much too large to be completely attributed to surface-atom core-level shifts which have been calculated to be 0.25 eV.² A leading peak is very evident in the $2p_{1/2}$ edge as well, though not as well resolved from the bulk peak because the $2p_{1/2}$ core level is intrinsically broader than the $2p_{3/2}$ level.³ As one lowers the detection threshold below the incident energy, electrons that have lost increasing amounts of energy are included, the sampling depth is increased, and the surface-state peak is steadily decreased relative to the bulk $2p_{3/2}$ peak. Finally, the limit in which one detects the total secondary electron yield (AEAPS) is illustrated by the spectrum in Fig. 4.

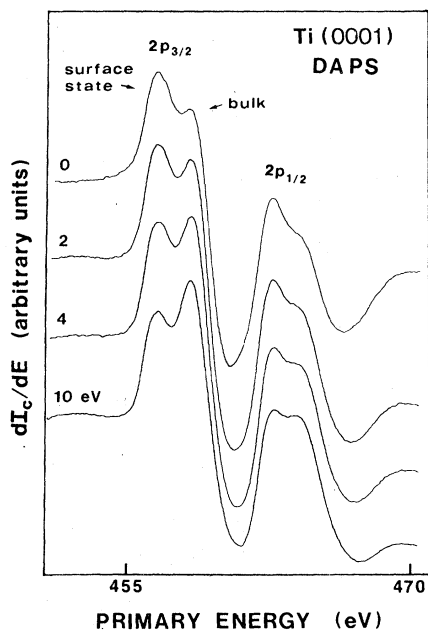


FIG. 3. Series of first-derivative disappearance potential spectra of the $2p$ levels of the clean Ti(0001) surface in which one collects secondary electrons that have lost up to 0, 2, 4, and 10 eV with respect to the incident electron energy (apart from a correction for the work function of the spectrometer). In the top spectrum one is detecting only the very-nearly-elastic secondaries, consequently emphasizing surface features. For the single-crystal surface, the surface states produce a leading peak in the $2p_{3/2}$ level larger than and well resolved from the bulk peak. The energy separation of these two peaks is ≈ 1.8 eV, too large to be attributed to surface-atom core-level shifts. As one increases the sampling depth by including increasingly inelastic secondaries, the surface-state peak is steadily decreased relative to the bulk $2p_{3/2}$ peak.

In this case the appearance potential spectrum has been inverted relative to the elastic yield spectrum (DAPS), since the total secondary yield increases at the threshold due to Auger recombination of the core hole, while the elastic yield decreases due to a new channel opening for inelastic processes.⁸ Note that there is little difference in the relative magnitudes of the surface state and $2p_{3/2}$ bulk peaks between this spectrum and the 10-eV (bottom) spectrum in Fig. 3, indicating that some limit in sampling depth has already been approached by including those secondaries whose energy is up to 10 eV below the primary energy.

The surface states also exhibit some degree of temperature dependence, as shown in Fig. 5. There is little change between the room-temperature appearance potential spectrum and the spectrum obtained with the sample at 150°C. As the sample

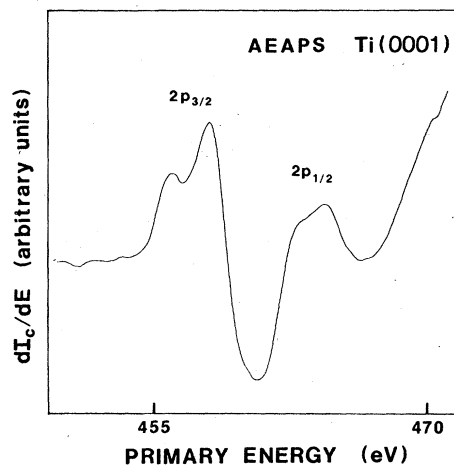


FIG. 4. First-derivative Auger electron appearance potential spectrum of the $2p$ levels of the clean Ti(0001) surface. In AEAPS one detects the total secondary-electron yield, and the sampling depth is determined by the energy of the incident electrons. At the $2P_{3/2}$ threshold (454.2 eV) this is approximately 5–10 Å. The AEAPS spectrum has been inverted relative to the elastic yield spectrum (DAPS), since the total secondary yield increases at the threshold while the elastic yield decreases.

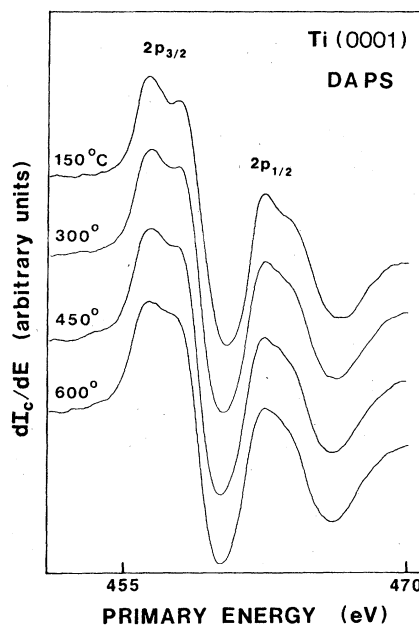


FIG. 5. Series of first-derivative disappearance potential spectra illustrating the temperature dependence of the surface states. As the sample temperature is increased the surface-state and bulk $2p_{3/2}$ peaks appear to broaden, until they overlap completely at 600°C. This is probably due to the thermal expansion of the crystal itself.

temperature is increased further, however, the surface state and $2p_{3/2}$ bulk peaks seem to broaden, until they overlap completely at 600 °C. This is probably due to the thermal expansion of the crystal itself—as the mean $\langle 0001 \rangle$ layer spacing increases, the surface-state peak in the LDOS of the first layer shown in Fig. 1 broadens, still apparent but far less prominent in an appearance potential spectrum.

IV. EFFECT OF OXYGEN

Appearance potential spectroscopy was used to follow changes in the surface electronic structure of the unfilled bands upon oxygen chemisorption. Figure 6 shows a series of first-derivative disappearance potential spectra (elastic yield) taken as a function of oxygen exposure, illustrating the sensitivity of the surface states to gas adsorption. The top spectrum is the clean-surface spectrum with the very prominent surface-state peak. In the same figure we show spectra for 1, 4, and finally 20 L ($1 \text{ L} = 10^{-6}$ Torr sec) exposure. By 20 L indicated exposure the surface-state peak is almost completely extinguished, and a shoulder on the trailing edge of both the $2p_{3/2}$ and $2p_{1/2}$ bulk peaks indicates that oxide formation has begun.¹³

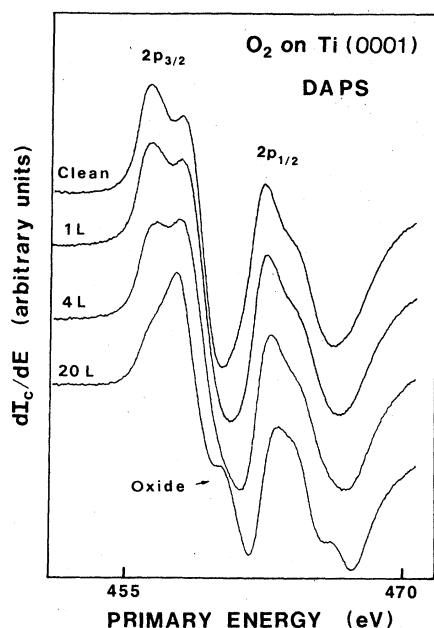


FIG. 6. Series of elastic yield spectra taken as a function of oxygen exposure, illustrating the rapid reduction of the surface-state peak with exposure. By 20 L the surface-state peak is almost completely extinguished, and a shoulder on the trailing edge of both the $2p_{3/2}$ and $2p_{1/2}$ bulk peaks indicate that oxide formation has begun.

LEED observations together with AES measurements were used to obtain an estimate of absolute oxygen coverage. Oxygen is known to produce a $p(2 \times 2)$ pattern on Ti(0001) which presumably corresponds to a $\frac{1}{4}$ -monolayer coverage. Shih *et al.*, however, have pointed out that a $p(2 \times 2)$ pattern can also be produced on this surface by the simultaneous presence of three $p(2 \times 1)$ oxygen domains 120° apart from one another.¹⁴ This situation corresponds to a $\frac{1}{2}$ -monolayer coverage. Consequently, one must rely on evidence other than the mere presence of the $p(2 \times 2)$ pattern to establish an absolute coverage. In practice, it is rather difficult to pinpoint the exposure at which maximum development of the $p(2 \times 2)$ pattern occurs. To facilitate the following discussion we choose to define a parameter R as the ratio of the oxygen (512 eV) to titanium (419 eV) peak-to-peak AES signals. Note that while R is proportional to coverage it is *not* the usual coverage parameter. After sputtering and annealing the sample, we obtained $R \approx 0.015$, similar to the results of Shih *et al.*¹⁰ This may correspond to residual oxygen which could not be removed by cleaning, or a titanium Auger line which happens to coincide with the oxygen line. If the peak is in fact due to residual oxygen, Shih *et al.* have estimated this to correspond to approximately 2% of a monolayer.¹⁰ LEED observations in this study revealed an initial formation of a very diffuse $p(2 \times 2)$ pattern upon exposing the room-temperature sample to oxygen up to $R = 0.04$. This diffuse pattern strengthened slightly with increasing exposure, appeared to reach maximum development at $R \approx 0.075$, and then gradually faded out and disappeared at $R = 0.09$. If the exposure is stopped at $R \approx 0.075$ and the sample is flashed to 250 °C, a well-ordered $p(2 \times 2)$ pattern is produced. This is accompanied by an abrupt change in the work function as discussed in a following paragraph. AES was used to monitor the actual relative amount of oxygen on the surface throughout the exposure up to 10 L. One might reasonably assume the sticking coefficient for oxygen to be relatively constant up to a coverage of $\frac{1}{4}$ monolayer, where it would be expected to change rather abruptly and then remain relatively constant again for increasing coverages until the chemical nature of the bond changes and an oxide begins to form. By measuring and plotting the oxygen AES signal as a function of exposure one can obtain an estimate of the exposure corresponding to a $\frac{1}{4}$ -monolayer coverage as evidenced by an abrupt change in slope. Several such series of measure-

ments were made with an observed change in slope occurring in each case at exposures corresponding to $R \approx 0.10$. We consider this to be in good agreement with the LEED observations, and believe that the evidence to date indicates that the $p(2 \times 2)$ pattern corresponds to a $\frac{1}{4}$ -monolayer coverage.

The work function is a very sensitive indicator of surface conditions for any metal. Existing published values made on titanium film, ribbon, field emission tip, and polycrystalline samples vary widely,¹⁵ due no doubt to the differences in surface morphology and varying degrees of surface contamination. Most recently, Feibelman and Himpsel have reported a value of 4.6 ± 0.1 eV for the (0001) surface using photoemission,⁶ in contrast to theoretical calculations by Feibelman *et al.* which predicted a value of only 3.8 eV for an 11-layer (0001) model film.² One of the authors, however, has noted that this is the least reliable result of their calculation.¹⁶ Accordingly, we have made experimental measurements of the work function for the clean and oxygen chemisorbed Ti(0001) single-crystal surface using the field-emission retarding potential (FERP) method as described in the literature.^{17,18}

In this technique, the sample surface is used as an equipotential momentum analyzer. When the potential difference between the sample and field-emission tip is just equal to the sample work function, electrons normally incident on the sample will arrive at the sample surface with zero kinetic energy if they have tunneled from the highest occupied level of the emitter. Thus, the potential difference between the field emitter and sample at the threshold for sample current, multiplied by the electronic charge, is an absolute measure of the sample work function. Since the tunneling probability of field emitted electrons drops off approximately exponentially for states below the Fermi level, the threshold is very sharp.

We obtain a clean surface work function of 4.58 ± 0.05 eV, in excellent agreement with that of Feibelman and Himpsel.⁶ As oxygen chemisorbs on the surface, the work function remains approximately constant for very low coverages and then steadily increases with additional exposure as shown in Fig. 7, where the change in work function $\Delta\phi$ is plotted versus R [R is the ratio of the AES oxygen (512 eV) to titanium (419 eV) peak-to-peak signals] up to a $R = 0.25$ (corresponding to approximately 10-L exposure) where the appearance potential spectrum begins to show evidence of oxide formation.¹³ The work function continues to increase with exposure, leveling off at a value of 5.3 eV as R ap-

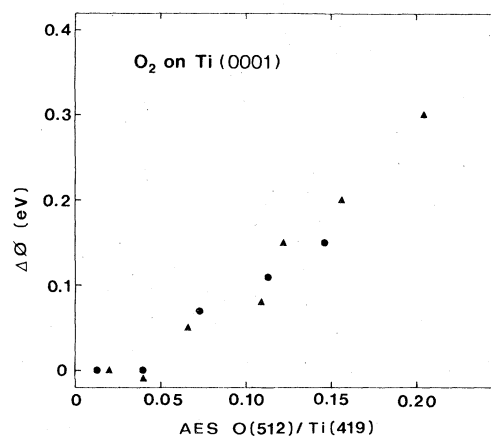


FIG. 7. The change in work function $\Delta\phi$ as a function of oxygen exposure. AES was used to monitor the actual relative amount of oxygen on the surface. We obtain a clean surface value of 4.58 ± 0.05 eV by the field-emission retarding potential (FERP) technique. The work function remained approximately constant for very low oxygen coverage, and then steadily increased with additional exposure, leveling off at approximately 5.3 eV as the surface became saturated.

proaches 0.45.

As noted earlier the $p(2 \times 2)$ LEED pattern obtained upon exposure at room temperature can be significantly improved by flashing the sample to 250 °C. This is accompanied by an abrupt decrease of 0.15 eV in the work function, although AES revealed no decrease in the amount of oxygen on the surface and no significant change was observed in the disappearance potential spectrum. Similar abrupt decreases in the work function were observed upon flashing the sample to 250 °C for other exposures as well, both before and after the presence of the $p(2 \times 2)$ superstructure. The magnitude of the decrease depended upon the amount of oxygen exposure since the last flash anneal cycle.

A typical series of measurements is as follows: exposing the clean, well-annealed room-temperature surface to oxygen up to $R = 0.032$ produces no observable change in the work function. However, flashing the sample to 250 °C at a rate of approximately 2 °C/sec and allowing it to cool to room-temperature results in a decrease of 0.07 eV, with no decrease in the oxygen AES signal. At this point a very broad and diffuse $p(2 \times 2)$ LEED pattern can be seen. If one increases the exposure the $p(2 \times 2)$ pattern gradually improves, although it remains rather diffuse, up to $R = 0.075$, after which it gradually fades out with increasing exposure. Halting the exposure at $R = 0.075$, the work func-

tion is seen to have increased by 0.05 eV from its last measured value. Flashing the sample to 250 °C at this point decreases the work function by 0.09 eV and significantly improves the $p(2 \times 2)$ pattern, producing a well-ordered structure in which the half-order beams are as sharp as the integral order beams (which remain sharp throughout the exposure). Increasing the exposure again to $R = 0.14$ results in a work function increase of 0.20 eV with a gradual increase in the LEED background intensity, while the $p(2 \times 2)$ half-order beams gradually broaden and disappear, never to reappear. Flashing the sample to 250 °C produces a decrease of 0.16 eV in the work function, with little if any improvement in the LEED pattern. With additional exposure the work function continues its cycle of increasing with exposure and abruptly decreasing upon a flash anneal.

This behavior indicates that there exists two distinct binding states of oxygen on the basal plane of titanium, with the higher energy " α state" corresponding to a lower work function. At low coverages oxygen is adsorbed preferentially in the α state, but with continued exposure more and more oxygen is adsorbed into a " β state" characterized by a work function higher than that of the clean surface. This appears to be confirmed by Hanson, Stockbauer, and Madey¹⁹ who report that electron or photon induced desorption from the low-coverage state of ox-

ygen on Ti(0001) is negligible. They find, however, that at small coverages the work function decreases as much as 0.13 eV below the clean surface values. An initial decrease in work function was also reported by Fukuda *et al.*⁵ and by Brearley and Surplice²⁰ for polycrystalline titanium. In the present study, the work function in the low-coverage region decreased below the clean-surface value only if the surface was flashed to a higher temperature. It appears therefore that although we are observing essentially the same phenomenon as Hanson *et al.*,¹⁹ a greater fraction of the adsorbed oxygen at low coverages is in the β state in our measurements. The reason for this difference may have to do with the details of surface morphology.

ACKNOWLEDGMENTS

We wish to thank Alan Melmed of the National Bureau of Standards and Len Beavis of Sandia Laboratories for providing the single-crystal samples used in the work reported here. D. M. Hanson, R. Stockbauer and T. E. Madey kindly made their results on electron and photon stimulated desorption of oxygen from the basal plane of titanium available to us prior to their publication. Helpful discussions with Peter J. Feibelman and D. R. Hamann are also gratefully acknowledged. This work supported by the National Science Foundation under Grant No. DMR-79-00323.

¹See, for example: C. S. Wang and A. J. Freeman, Phys. Rev. B **19**, 793 (1979).

²Peter J. Feibelman, J. A. Appelbaum, and D. R. Hamann, Phys. Rev. B **20**, 1433 (1979).

³Robert L. Park and J. E. Houston, Phys. Rev. B **6**, 1073 (1972).

⁴C. Nyberg, Surf. Sci. **52**, 1 (1975).

⁵Y. Fukuda, W. T. Elam, and Robert L. Park, Appl. Surf. Sci. **1**, 278 (1978).

⁶Peter J. Feibelman and F. J. Himpsel, Phys. Rev. B **21**, 1394 (1980).

⁷Robert L. Park and J. E. Houston, J. Vac. Sci. Technol. **11**, 1 (1974).

⁸M. L. denBoer, Phillip I. Cohen, and Robert L. Park, Surf. Sci. **70**, 643 (1978).

⁹J. Kirschner and P. Staib, Phys. Lett. **42A**, 335 (1973).

¹⁰H. D. Shih, F. Jona, D. W. Jepsen, and P. M. Marcus, J. Phys. C **9**, 1405 (1976).

¹¹C. R. Brundel, Surf. Sci. **48**, 99 (1975).

¹²J. Kirschner and P. Staib, Appl. Phys. **6**, 99 (1975).

¹³Robert L. Park and J. E. Houston in *Advances in X-ray Analysis*, edited by Kurt F. J. Heinrich, Charles S. Barret, John B. Newkirk, and Clayton O. Ruud (Plenum, New York, 1971), Vol. 15, pp. 462–469.

¹⁴H. D. Shih, F. Jona, D. W. Jepsen, and P. M. Marcus, J. Vac. Sci. Technol. **15**, 596 (1978).

¹⁵R. J. D'Arcy and N. A. Surplice, Surf. Sci. **36**, 783 (1973).

¹⁶Peter J. Feibelman, private communication.

¹⁷J. E. Henderson and R. E. Badgley, Phys. Rev. **38**, 590 (1931).

¹⁸R. W. Strayer, W. Mackie, and L. W. Swanson, Surf. Sci. **34**, 225 (1973).

¹⁹D. M. Hanson, R. Stockbauer, and T. E. Madey, Appl. Surf. Sci. (in press.)

²⁰W. Brearley and N. A. Surplice, Surf. Sci. **64**, 372 (1977).